Analytical Methods

COMMUNICATION

Cite this: *Anal. Methods*, 2018, **10**, 2303

Received 16th March 2018
Accepted 19th April 2018

DOI: 10.1039/c8ay00568k

rsc.li/methods

Discrimination of positional isomers by ion mobility mass spectrometry: application to organic semiconductors†

Quentin Duez,[ab] Maxime Romain,[c] Corentin Tonneaux,[ab] Julien De Winter,[a] Vincent Lemaur,[b] Jérôme Cornil,*[b] Cyril Poriel*[c] and Pascal Gerbaux*[a]

Organic semiconductors are increasingly being used in organic-based opto-electronic devices. Since regioselective synthetic approaches are not always controlled, promising compounds are sometimes prepared following non-regioselective routes. Ion mobility mass spectrometry is here introduced as a direct method to distinguish isomers in mixtures, instead of undertaking time-consuming analytical chromatography procedures.

Positional isomerism is nowadays an important molecular tool to tune the electronic properties of organic materials of interest in the field of organic electronics.[1,2] In this context, dihydroindenofluorene regioisomers have recently emerged as an interesting family of organic semiconductors, which can be used as efficient fluorescent emitters in Organic Light-Emitting Diodes (OLEDs),[3] host materials for phosphorescent OLEDs,[4] electron acceptors for non-fullerene organic solar cells[5] and electron transporters in Organic Field-Effect Transistors (OFETs).[6] From a structural point of view, within the dihydroindenofluorene family, different positional isomers can be generated with different phenylene linkages (*para*/*meta*) or ring bridging geometries (*anti vs. syn*). 6,12-dihydroindeno[1,2-*b*]fluorene has been the first and most studied isomer[7,8] while the other isomers remain scarcely used. Antiaromatic indenofluorene regioisomers have also been widely developed in recent years.[9] Many synthetic strategies have been explored in the past few years for the efficient preparation of dihydroindenofluorene isomers, using regioselective routes[10] or not.[3,11] The non-regioselective approaches reported in the literature present advantages leading to the simultaneous formation of two different regioisomers, which is an appealing feature provided that their detection and separation is possible. In 2009, an efficient and versatile synthesis of dihydroindeno[1,2-*b*]fluorene (*anti*) and dihydroindeno[2,1-*a*]fluorene (*syn*) positional isomers was reported (Scheme S1, ESI1†).[11] In order to avoid a time-consuming chromatographic separation to isolate the pure regioisomers, rational ways of favouring the formation of one given isomer have been investigated, with special attention given to the solvent and temperature conditions.[10] Strategies to quickly and efficiently reveal the presence of positional dihydroindenofluorene isomers within a crude mixture would represent a useful asset on the way to their development. The present work demonstrates that this can be fulfilled by Ion Mobility Mass Spectrometry (IMMS).

Single-stage mass spectrometry cannot detect the presence of positional isomers due to their identical elemental composition. On the other hand, ion mobility separation represents an elegant method to discriminate and identify the corresponding regioisomeric ions. IMMS is increasingly being used within the mass spectrometry community for probing the 3D structures of gaseous ions. This methodology allows for the temporal separation of ions based on their mobility in a cell filled with a buffer gas (He or N_2) under the influence of an electric field. The drift time (t_D) of the ions across the mobility cell is directly proportional to their collisional cross section (CCS) which reflects the three-dimensional shape of the ions in the gas phase.[12] Over the past few years, this analytical dimension was proven effective, in combination with computational chemistry, for the structural characterization of a large range of compounds such as (bio) macromolecules,[13–15] host–guest systems[16] and molecular switches.[17,18] IMMS was also used for the temporal separation of isomeric species, such as glycans,[19–21] peptides,[22,23] oligosaccharides,[24] and saponins,[25] derived from natural matrices. The originality of the present work is to demonstrate the applicability of the IMMS approach to the realm of organic semiconductors not only to separate isomers but also to identify their structures by exploiting a deep synergy with computational modelling.

[a]*Organic Synthesis and Mass Spectrometry Laboratory, Interdisciplinary Center for Mass Spectrometry (CISMa), Center of Innovation and Research in Materials and Polymers (CIRMAP), University of Mons – UMONS, 23 Place du Parc, 7000 Mons, Belgium. E-mail: pascal.gerbaux@umons.ac.be*

[b]*Laboratory for Chemistry of Novel Materials, Center of Innovation and Research in Materials and Polymers (CIRMAP), University of Mons – UMONS, 23 Place du Parc, 7000 Mons, Belgium. E-mail: jerome.cornil@umons.ac.be*

[c]*Univ Rennes, CNRS, ISCR-UMR 6226, F-35000 Rennes, France. E-mail: cyril.poriel@univ-rennes1.fr*

† Electronic supplementary information (ESI) available. See DOI: 10.1039/c8ay00568k

Dihydroindenofluorene isomer mixtures were diluted in acetonitrile and subsequently ionized and transferred to the gas phase of a mass spectrometer using an Electrospray Ionization (ESI) ion source. All results presented hereafter are related to radical cations that are readily produced upon ESI by the removal of one electron. The ion mobility data are represented in terms of CCS distributions determined on the basis of arrival time distributions (ATD) using a suitable calibration procedure recently developed in Mons.[26] Note that each experiment described in the present paper was performed three times using different ion mobility settings (see the ESI†) to ensure the robustness of the method. The presented CCSs are mean values with standard deviations in brackets.

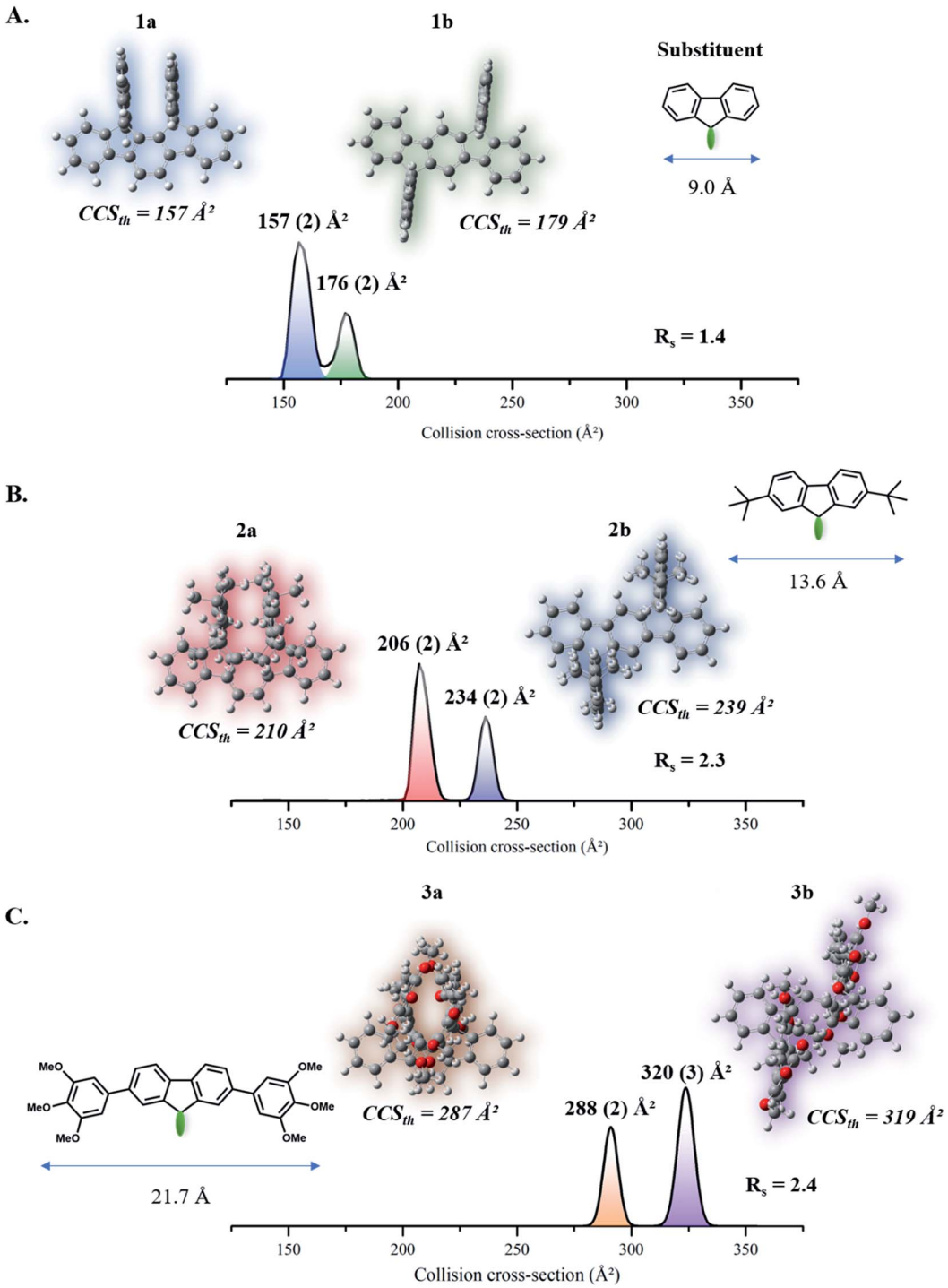

Fig. 1 (A, B and C) Experimental and theoretical CCS values for **1a**/**1b**, **2a**/**2b** and **3a**/**3b** radical cations. The green dots represent the location of the terphenylene core. The lengths of the substituents were theoretically extracted from the optimized geometries of each substituent, and they are also displayed. The presented CCSs are mean values with standard deviations in brackets.

The synthesis of compounds combining the bridged *p*-terphenylene core and two fluorene moieties through spiro-linkages yields a mixture of *syn* and *anti* (**1a** and **1b** in Fig. 1A, respectively) isomers.[11] When the isomer mixture is subjected to ion mobility experiments, a bimodal distribution (*i.e.*, two ion families) is observed for the mass-to-charge ratio corresponding to the cation radical isomers and might correspond to the two separated isomers, to conformers or even to contaminants. In order to assess whether the two distributions correspond to the two ionized isomers and to unambiguously assign the peaks observed in the mobilograms, the geometries of the corresponding radical cations have been optimized at the quantum-chemical level and their CCS calculated using the widely used trajectory method model, as implemented in Collidoscope[27] (Fig. 1A). The excellent agreement between the experimental and theoretical CCS values (<3% difference) confirms that the *syn* (**1a**) isomer is associated with the lower CCS distribution while the *anti* (**1b**) isomer generates the higher CCS distribution. The peak separation efficiency in ion mobility spectrometry can be quantified by associating the peak full width at half maximum values (ω_A and ω_B) and the peak separation ($t_B - t_A$) into a resolution parameter, R_s, defined by the following equation:[28]

$$R_s = 1.18\ \frac{t_B - t_A}{\omega_A + \omega_B}$$

We have used here a variant of this definition by injecting the average CCS values and the width at half maximum ΔCCS:[28]

$$R_s = 1.18\frac{CCS_B - CCS_A}{\Delta CCS_A + \Delta CCS_B}$$

For the **1a**/**1b** isomer pair, we measured the R_s, which amounted to 1.4 and reflected the small signal overlap observed in the mobilograms (see Fig. 1A). In peak separation theory, for two peaks with Gaussian distributions and the same heights/widths, a resolution of 1.5 corresponds to an overlap of less than 0.15%.[29]

When comparing the optimized structures of **1a**/**1b** radical cations, the CCS difference can be clearly associated with the relative orientation of the substituents. We thus anticipate that the R_s value will be affected by the size of the substituents. Accordingly, we have next applied our IMS/quantum chemistry association to the **2a**/**2b**[30] and **3a**/**3b**[19] isomer pairs exhibiting bulkier substituents on the fluorene units (*tertio*-butyl and 3,4,5-trimethoxyphenyl groups, respectively, Fig. 1B and C). The results indicate that the *syn* isomer radical cations are always characterized by the smaller CCS, *i.e.*, the more compact structures. Moreover, the CCS_{exp} increases with the substituent size, with values of 157/176 Å^2, 206/234 Å^2, and 288/320 Å^2 for the **1a**/**1b**, **2a**/**2b** and **3a**/**3b** isomer pairs, respectively. The deep correlation between the CCS_{exp} and CCS_{th} values is remarkable, leading to the straightforward identification of the isomers. As expected, the bulkier the substituent, the better is the separation efficiency, with R_s measured to be 2.3 and 2.4 for the **2a**/**2b** and **3a**/**3b** isomer pairs, respectively, a value which is usually associated with a baseline separation.[28] The applicability of

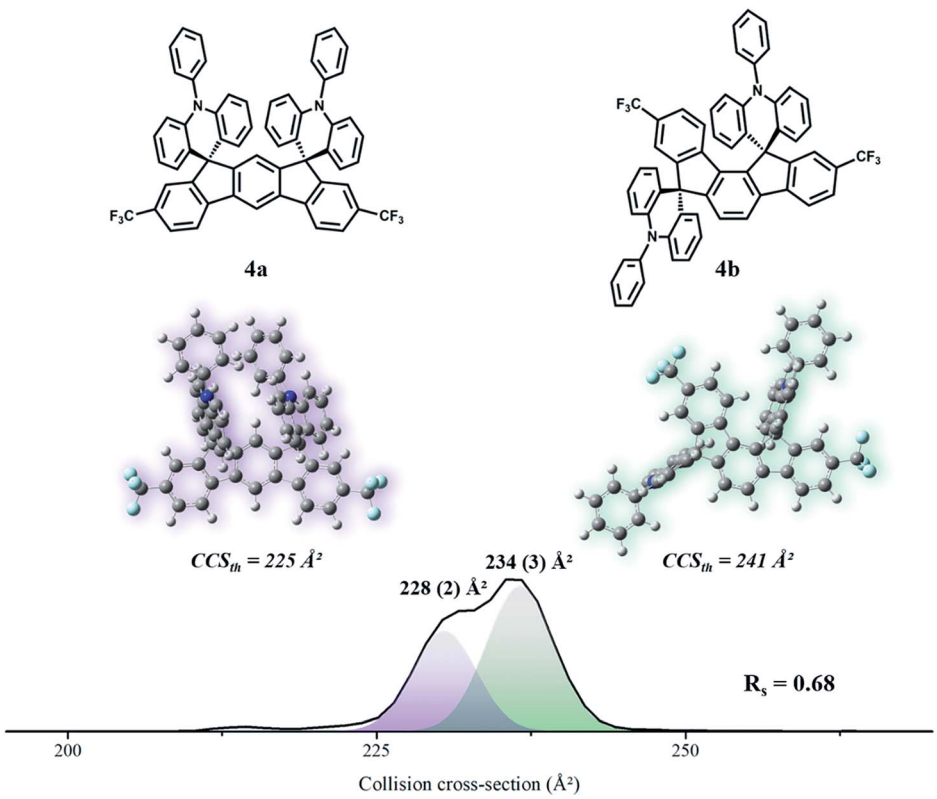

Fig. 2 Experimental and theoretical CCS values for isomers **4a**/**4b**. The presented CCSs are mean values with the standard deviations in brackets.

IMMS is not limited to fluorene substituents and to *p*-terphenylene backbones, as shown below by the investigation of more elaborate structures. These molecules (**4a** and **4b** in Fig. 2) consist of an *m*-terphenylene core substituted by spiro-linked phenylacridine units.[4] Here, the separation efficiency is less pronounced, yielding an asymmetric CCS distribution and a lower R_s factor value of 0.68 (Fig. 2). Upon Gaussian deconvolution and comparison between CCS_{exp} and CCS_{th} values, it appears that these two distributions do correspond to each regioisomer radical cation. Based on the results obtained with sterically encumbered substituents on the *p*-terphenylene cores, the separation efficiency is expected to be enhanced with bulkier substituents under our experimental conditions.

In summary, we have illustrated that IMMS can be advantageously used to readily detect isomers of organic semiconductors produced simultaneously in chemical reactions. This is another successful application of the IMMS technique which is here supplemented by an intimate coupling to computational chemistry allowing for the structural assignment of the IMMS signals. This original joint theoretical and experimental approach is versatile and should find application in many other research areas. The exact quantification of both isomers in the starting mixture could be estimated based on our IMMS measurements, provided that the ionization cross sections for both isomers – *i.e.*, the mathematical relation between the ion abundance in the IMMS spectrum and the concentration in the solution phase – can be determined by a calibration procedure; this issue is beyond the scope of the present paper. Although most current commercial IMMS setups can only be exploited to detect isomers with sufficient structural differences due to the inherent instrumental resolution, we are convinced that the recent development of high resolution ion mobility instruments will reinforce the use of ion mobility technology as a routine analytical tool within the organic synthesis community to detect isomeric products and to optimize (non)-regioselective synthetic routes.

Conflicts of interest

There are no conflicts to declare.

Notes and references

1 M. Romain, S. Thiery, A. Shirinskaya, C. Declairieux, D. Tondelier, B. Geffroy, O. Jeannin, J. Rault-Berthelot, R. Métivier and C. Poriel, *Angew. Chem., Int. Ed.*, 2015, **54**, 1176–1180.

2 J. D. Peltier, B. Heinrich, B. Donnio, O. Jeannin, J. Rault-Berthelot and C. Poriel, *Chem.–Eur. J.*, 2017, **23**, 17290–17303.

3 M. Romain, D. Tondelier, J. Vanel, B. Geffroy, O. Jeannin, J. Rault-Berthelot, R. Métivier and C. Poriel, *Angew. Chem., Int. Ed.*, 2013, **52**, 14147–14151.

4 M. Romain, D. Tondelier, B. Geffroy, O. Jeannin, E. Jacques, J. Rault-Berthelot and C. Poriel, *Chem.–Eur. J.*, 2015, **21**, 9426–9439.

5 D. Xia, D. Gehrig, X. Guo, M. Baumgarten, F. Laquai and K. Müllen, *J. Mater. Chem. A*, 2015, **3**, 11086–11092.

6 M. Romain, M. Chevrier, S. Bebiche, T. Mohammed-Brahim, J. Rault-Berthelot, E. Jacques and C. Poriel, *J. Mater. Chem. C*, 2015, **3**, 5742–5753.

7 H. Reisch, U. Wiesler, U. Scherf and N. Tuytuylkov, *Macromolecules*, 1996, **29**, 8204–8210.

8 S. Setayesh, D. Marsitzky and K. Müllen, *Macromolecules*, 2000, **33**, 2016–2020.

9 C. K. Frederickson, B. D. Rose and M. M. Haley, *Acc. Chem. Res.*, 2017, **50**, 977–987.

10 D. Thirion, C. Poriel, J. Rault-Berthelot, F. Barrière and O. Jeannin, *Chem.–Eur. J.*, 2010, **16**, 13646–13658.

11 C. Poriel, F. Barrière, D. Thirion and J. Rault-Berthelot, *Chem.–Eur. J.*, 2009, **15**, 13304–13307.

12 F. Lanucara, S. W. Holman, C. J. Gray and C. E. Eyers, *Nat. Chem.*, 2014, **6**, 281–294.

13 H. Metwally, R. G. Mcallister, V. Popa and L. Konermann, *Anal. Chem.*, 2016, **88**, 5345–5354.

14 Q. Duez, T. Josse, V. Lemaur, F. Chirot, C. M. Choi, P. Dubois, P. Dugourd, J. Cornil, P. Gerbaux and J. De Winter, *J. Mass Spectrom.*, 2017, **52**, 133–138.

15 W. Zhang, A. Abdulkarim, F. E. Golling, H. J. Räder and K. Müllen, *Angew. Chem.*, 2017, **129**, 2645–2648.

16 G. Carroy, V. Lemaur, C. Henoumont, S. Laurent, J. De Winter, E. De Pauw, J. Cornil and P. Gerbaux, *J. Am. Soc. Mass Spectrom.*, 2018, **29**, 121–132.

17 L. H. Urner, B. N. S. Thota, O. Nachtigall, S. Warnke, G. von Helden, R. Haag and K. Pagel, *Chem. Commun.*, 2015, **51**, 8801–8804.

18 J. N. Bull, E. Carrascosa, N. Mallo, M. S. Scholz, G. da Silva, J. E. Beves and E. J. Bieske, *J. Phys. Chem. Lett.*, 2018, 7b03402.

19 F. Zhu, S. Lee, S. J. Valentine, J. P. Reilly and D. E. Clemmer, *J. Am. Soc. Mass Spectrom.*, 2012, **23**, 2158–2166.

20 M. D. Plasencia, D. Isailovic, S. I. Merenbloom, Y. Mechref and D. E. Clemmer, *J. Am. Soc. Mass Spectrom.*, 2008, **19**, 1706–1715.

21 Y. Yamaguchi, W. Nishima, S. Re and Y. Sugita, *Rapid Commun. Mass Spectrom.*, 2012, **26**, 2877–2884.

22 A. J. Creese and H. J. Cooper, *J. Am. Soc. Mass Spectrom.*, 2016, **27**, 2071–2074.

23 C. A. Srebalus Barnes, A. E. Hilderbrand, S. J. Valentine and D. E. Clemmer, *Anal. Chem.*, 2002, **74**, 26–36.

24 S. Poyer, C. Lopin-Bon, J. C. Jacquinet, J. Y. Salpin and R. Daniel, *Rapid Commun. Mass Spectrom.*, 2017, **31**, 2003–2010.

25 C. Decroo, E. Colson, M. Demeyer, V. Lemaur, G. Caulier, I. Eeckhaut, J. Cornil, P. Flammang and P. Gerbaux, *Anal. Bioanal. Chem.*, 2017, **409**, 3115–3126.

26 Q. Duez, F. Chirot, R. Liénard, T. Josse, C. Choi, O. Coulembier, P. Dugourd, J. Cornil, P. Gerbaux and J. De Winter, *J. Am. Soc. Mass Spectrom.*, 2017, **28**, 2483–2491.

27 S. A. Ewing, M. T. Donor, J. W. Wilson and J. S. Prell, *J. Am. Soc. Mass Spectrom.*, 2017, **28**, 587–596.

28 J. N. Dodds, J. C. May and J. A. McLean, *Anal. Chem.*, 2017, **89**, 12176–12184.

29 L. S. Ettre, *Pure Appl. Chem.*, 1993, **65**, 819–872.

30 D. Thirion, C. Poriel, F. Barrière, R. Métivier, O. Jeannin and J. Rault-Berthelot, *Org. Lett.*, 2009, **11**, 4794–4797.

